

Supporting Information

Satellite-like Gold Nanocomposites for Targeted Mass Spectrometry Imaging of Tumor Tissues

Yu-Ting Tseng¹, Scott G. Harroun², Chien-Wei Wu¹, Ju-Yi Mao³, Huan-Tsung Chang^{1,4}✉, and

Chih-Ching Huang^{3,5,6}✉

1. Department of Chemistry, National Taiwan University, Taipei, 10617, Taiwan
2. Department of Chemistry, Université de Montréal, Montréal, Québec, H3C 3J7, Canada
3. Department of Bioscience and Biotechnology, National Taiwan Ocean University, Keelung, 20224, Taiwan
4. Department of Chemistry, Chung Yuan Christian University, Taoyuan City, 32023, Taiwan.
5. Center of Excellence for the Oceans, National Taiwan Ocean University, Keelung, 20224, Taiwan
6. School of Pharmacy, College of Pharmacy, Kaohsiung Medical University, Kaohsiung, 80708, Taiwan

✉ Corresponding author: Huan-Tsung Chang, Department of Chemistry, National Taiwan University, 1, Section 4, Roosevelt Road, Taipei 10617, Taiwan; tel. and fax: 011-886-2-3366-1171; e-mail: changht@ntu.edu.tw; Chih-Ching Huang, Department of Bioscience and Biotechnology, National Taiwan Ocean University, 2, Beining Road, Keelung 20224, Taiwan; tel.: 011-886-2-2462-2192 ext 5517; fax: 011-886-2-2462-2320; e-mail: huanging@ntou.edu.tw

EXPERIMENTAL

Materials. AS1411 aptamer was purchased from Integrated DNA Technologies (Coralville, IA, USA). Tetrachloroauric(III) acid was purchased from Acros (Geel, Belgium). Sodium phosphate tribasic, sodium phosphate dibasic, tris-base, acetic acid, potassium chloride, magnesium chloride, calcium chloride, bovine serum albumin (BSA), xylene, ethanol, hematoxylin, citric acid, acetic acid, calcium chloride and isopropanol were purchased from Sigma-Aldrich (St. Louis, MO, USA). Fetal bovine serum (FBS), antibiotic-antimycotic solution, L-glutamine, nonessential amino acid solution, DMEM, RPMI-1640 and α -MEM cell culture media were purchased from Gibco BRL (Grand Island, NY, USA). OliGreen was purchased from Molecular Probes (Thermo Fisher Scientific Inc., Eugene, OR, USA). Human breast adenocarcinoma cell lines (MDA-MB-231 and MCF-7) and normal mammary epithelial cell line (MCF-10A) were obtained from the American Type Culture Collection (Manassas, VA, USA). The nucleolin antibody (C23(D-6)) was purchased from Santa Cruz Biotechnologies (Santa Cruz, CA, USA). Anti-mouse IgG and HRP-linked antibody were purchased from Cell Signaling Technology (Danvers, MA, USA). The ultraView Universal DAB Detection Kit was purchased from Ventana Medical Systems (Tucson, AZ, USA). Human normal breast tissue section (BRE01) and human breast cancer section (BRE06) were used for tissue imaging under formalin-fixed and paraffin-embedded conditions were purchased from Pantomics Inc (Richmond, CA, USA). A Milli-Q ultrapure water purifier from Millipore (Billerica, MA, USA) was used to produce ultrapure DI water (18.2 M Ω ·cm).

Preparation of 13-nm spherical Au NPs. Aqueous 4.0 mM trisodium citrate (50 mL) was brought to a vigorous boil while stirring in a round-bottom flask fitted with a reflux condenser. HAuCl₄ (1.0 mM, 0.5 mL) was added rapidly and then the mixture was heated for another 8 min, during which time the color changed from pale yellow to deep red. The solution was cooled to room temperature with continuous stirring. TEM revealed nearly monodisperse Au NPs having an average size of 13.3 \pm 1.2 nm. A double-beam UV–Vis spectrophotometer (Cintra 10e, GBC, Victoria, Australia) was used to measure the absorption of the Au NP solution. The particle concentration of the Au NPs (15 nM) was determined according to Beer's law using an extinction

coefficient of $2.43 \times 10^8 \text{ M}^{-1} \text{ cm}^{-1}$ at 520 nm for 13.3-nm Au NPs.

Cell Culture and Cytotoxicity Assays. MCF-7 cells were cultured in RPMI medium supplemented with fetal bovine serum (10%), antibiotic–antimycotic (1.0%). MDA-MB-231 cells were maintained in DMEM supplemented with FBS (10%), antibiotic–antimycotic (1.0%), L-glutamine ($2.0 \times 10^{-3} \text{ M}$), and nonessential amino acids (1.0%). MCF-10A cells were cultured in α -MEM supplemented with FBS (10%), and antibiotic–antimycotic (1.0%). All cells were cultured in an environment equilibrated with 5% CO_2 at 37 °C. The cell number and viability of the cells were determined by applying the trypan blue exclusion method and Alamar Blue assay, respectively. Following the separated incubation of MCF-7, MDA-MB-231 and MCF-10A cells (5.0×10^4 cells per well) in a culture medium for 24 h at 37 °C containing 5% CO_2 , each of the culture media were replaced with 500 μL of cell culture medium containing AS1411–Au NPs/Au@PC NPs, and then further cultured for an additional 24 h. The cells were carefully rinsed thrice with biological solution, and then reacted with Alamar Blue reagent for 2 h. Fluorescence of the as-formed reduced dye was measured using a Synergy H1 Multi-Mode Microplate Reader (Biotek Instruments), with an excitation wavelength of 545 nm and an emission wavelength of 590 nm. Because fluorescence intensity is directly correlated with cell quantity, cell viability was calculated by assuming 100% viability in the control set (media without nanoparticles).

Immunohistochemistry with horseradish peroxidase. First, the paraffin-embedded tissue sections are deparaffinized by soaking of tissue samples in xylene (99%) for 10 min, and then placed in fresh xylene and incubated for another 10 min; they were immersed sequentially in 100, 95, and 70% EtOH (5 min each). Then, the surfaces of the slides were cleaned with deionized water. The sandwich assay was conducted by following the first antibody (nucleolin mouse antibody), second antibody (anti-mouse IgG), and HRP-linked antibody. The staining reagents were 3,3-diaminobenzidine tetrahydrochloride and hematoxylin. HRP oxidized 3,3-diaminobenzidine tetrahydrochloride to stain the location of the antibody in the form of dark brown-colored products. Hematoxylin was used to stain the nuclei with blue color.

Table S1. Size and optical properties of as-synthesized Au@PC NP under various conditions.

Sample Number	pH ^a	Ratio ([catechin]/[HAuCl ₄])	[HAuCl ₄] (mM)	Core diameter (nm) ^b	Shell thickness (nm) ^c	Hydrodynamic diameter (nm) ^d	Zeta potential (mV) ^e	A _{max} (nm) ^f	FWHM (nm) ^g
1	3.0	1.0	0.5	73 ± 12	54 ± 10	142 ± 35	-30.1	575	120
2	5.0	1.0	0.5	46 ± 25	45 ± 22	93 ± 40	-37.3	-	-
3	7.0	1.0	0.5	25 ± 5, 142 ± 28	10 ± 5, 97 ± 45	186 ± 115	-36.3	-	-
4	9.0	1.0	0.5	8 ± 3	-	12 ± 8	-38.0	-	-
5	3.0	0.1	0.5	92 ± 23	-	107 ± 52	-28.2	550	70
6	3.0	0.2	0.5	78 ± 21	15 ± 5	122 ± 42	-27.7	568	90
7	3.0	2.0	0.5	30 ± 15	12 ± 8	310 ± 95	-31.2	-	-
8	3.0	4.0	0.5	33 ± 18	10 ± 6	355 ± 152	-20.5	-	-
9	3.0	1.0	0.1	30 ± 16	33 ± 12	105 ± 15	-28.6	-	-
10	3.0	1.0	1.0	250 ± 53	107 ± 25	312 ± 98	-32.4	730	250
11	3.0	1.0	5.0	356 ± 152	110 ± 52	450 ± 195	-28.0	-	-

^a Tris-acetate buffer solution (10 mM). ^{b,c} The results were obtained by TEM. ^{d,e} The results were obtained by dynamic light scattering. ^f Absorption maximum at surface plasmon resonance (SPR) of gold nanoparticles. ^g Full width at half maximum of SPR band.

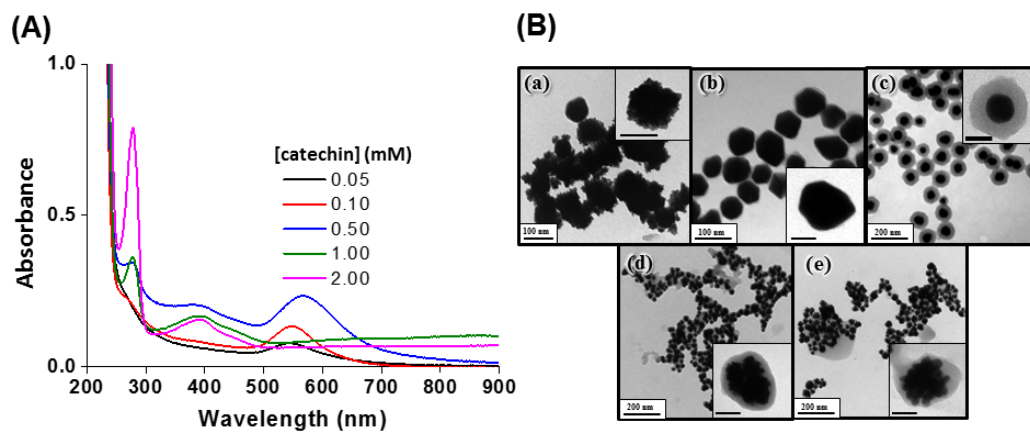


Figure S1. (A) UV-vis absorption spectra and (B) TEM images of the Au@PC NPs synthesized from HAuCl₄ (0.5 mM) and (a) 0.05 mM, (b) 0.10 mM, (c) 0.50 mM, (d) 1.00 mM, and (e) 2.00 mM catechin in Tris-acetate buffer solution (10 mM, pH 3.0). Insets to (B) are the corresponding high-magnification TEM images. The scale bars in the insets represent (a) 100 nm, (b) 20 nm, (c) 50 nm, (d) 15 nm, and (e) 15 nm.

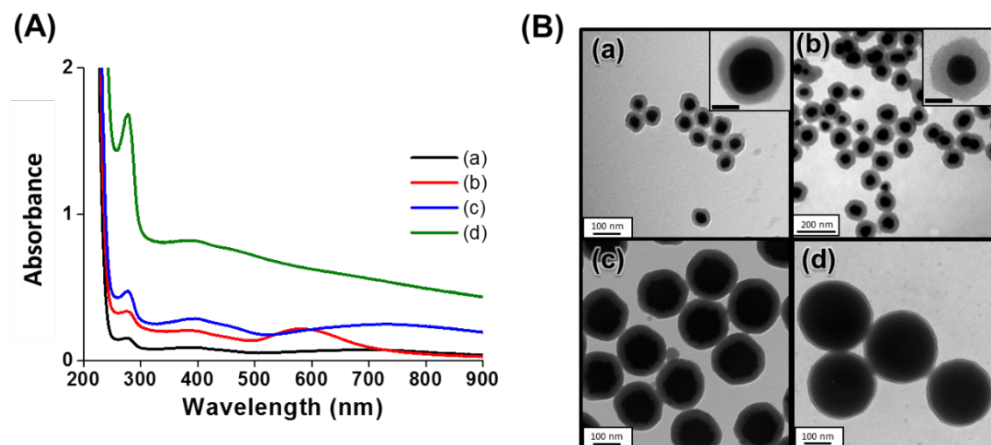


Figure S2. (A) UV-vis absorption spectra and (B) TEM images of the Au@PC NP synthesized using various concentrations of catechin and H_{AuCl₄} in Tris-acetate buffer solution (10 mM, pH 3.0). [Catechin] = [H_{AuCl₄}] = (a) 0.1 mM, (b) 0.5 mM, (c) 1.0 mM, and (d) 5.0 mM. Insets to (B) are the corresponding high-magnification TEM images. The scale bars in the inset represent (a) 20 nm and (b) 50 nm.

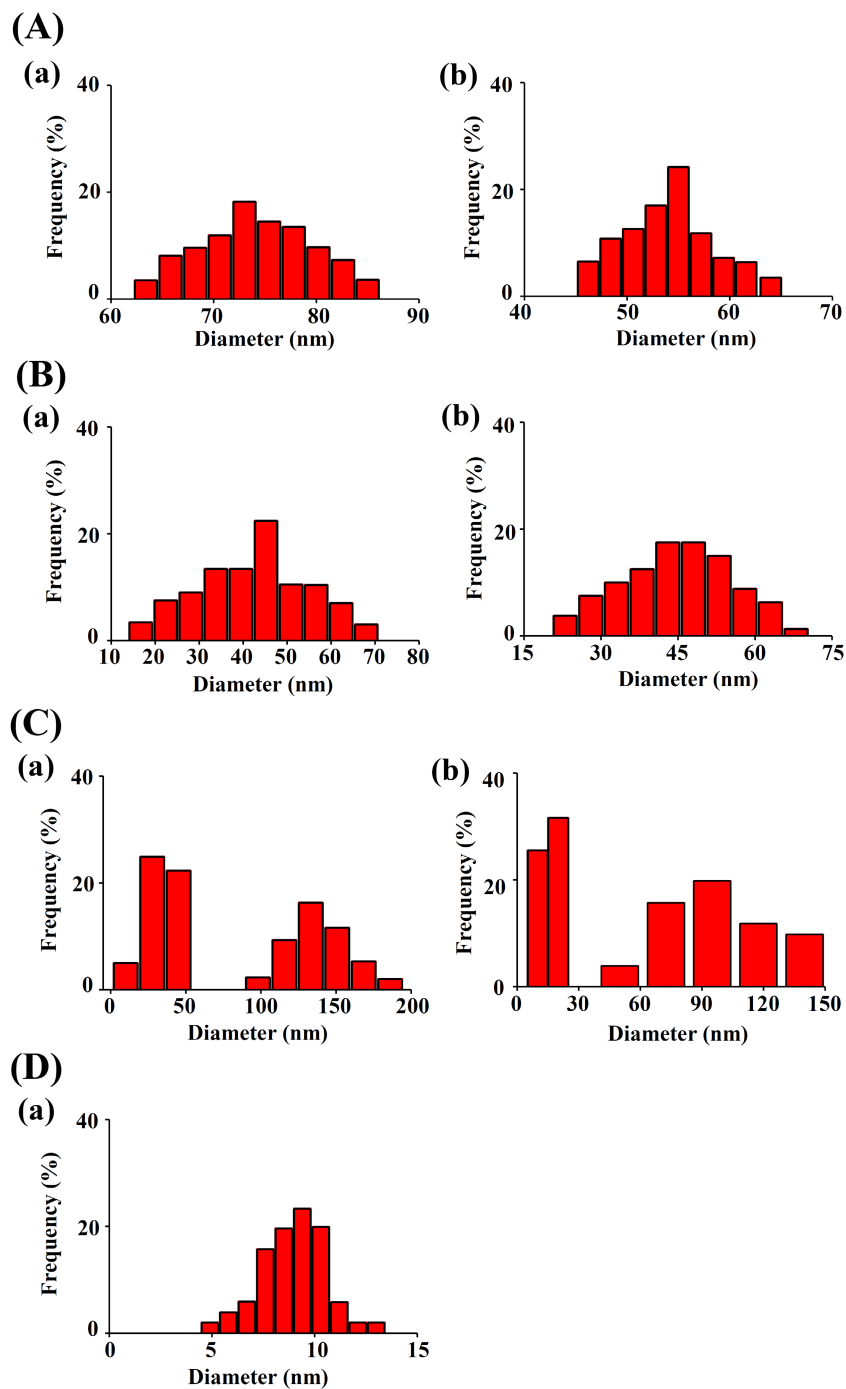


Figure S3. The histograms of the (a) core and (b) shell thickness distribution (each calculated from 100 counts) of the Au@PC NPs synthesized from 0.5 mM HAuCl₄ and 0.5 mM catechin in Tris-acetate buffer solution (10 mM) at (A) pH 3.0, (B) pH 5.0, (C) pH 7.0, and (D) pH 9.0.

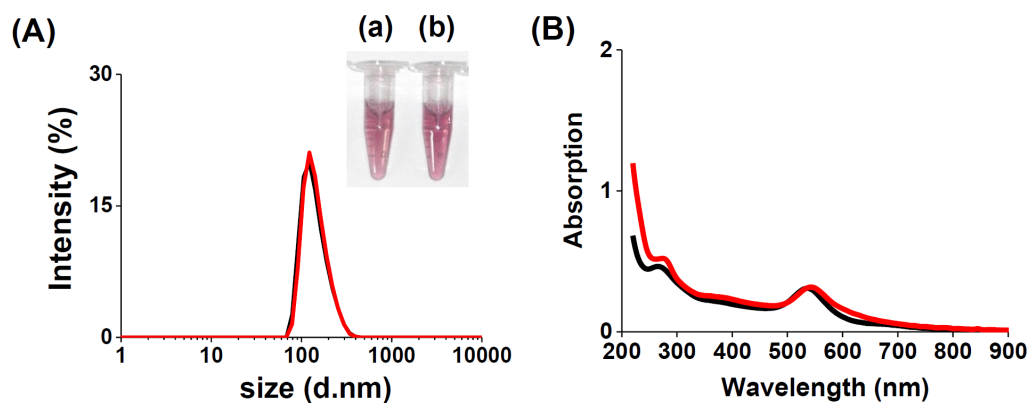


Figure S4. (A) DLS spectra and (B) UV-vis absorption spectra of purified Au@PC NPs (2-fold diluted) prepared in (black) DI water and (red) biological mimetic solution. Inset: photograph of corresponding Au@PC NPs in (a) DI water and (b) biological mimetic solution. The DLS bands of these two prepared Au@PC NP samples are both approximately 140 nm. The UV-Vis spectra show an absorption peak at 575 nm for each of the two prepared Au@PC NP samples, which can be attributed to absorption by the dispersed Au NPs. Our results indicate that the Au@PC NP were stable (no aggregation) in biological mimetic solution.

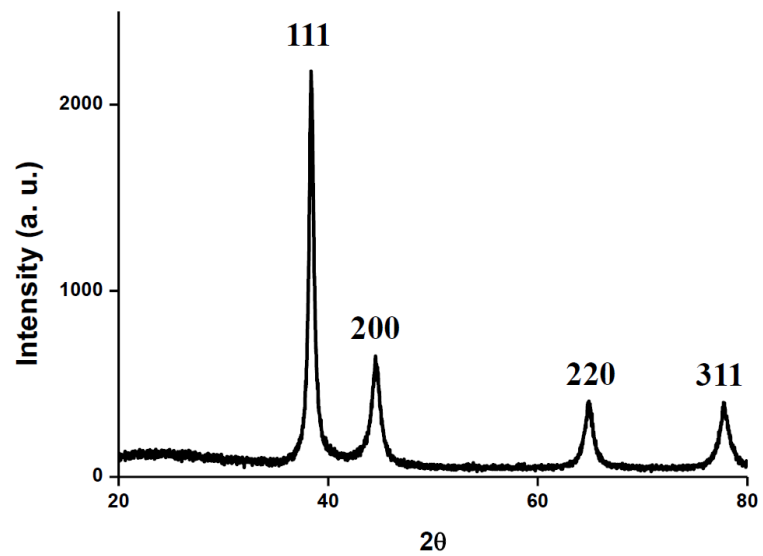


Figure S5. XRD patterns of the Au@PC NPs.

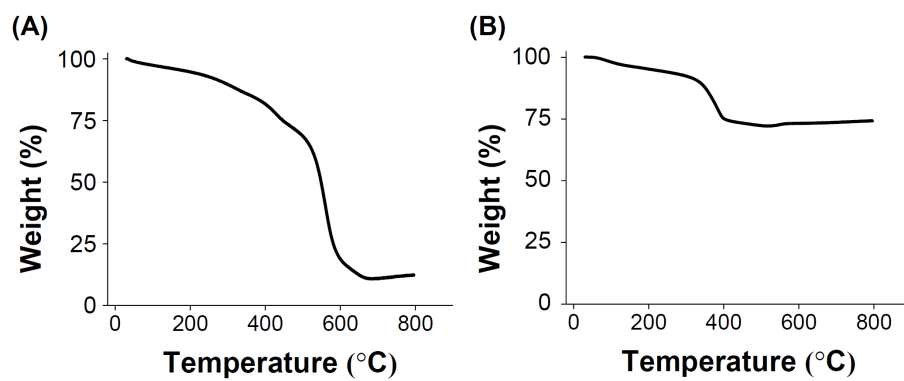


Figure S6. TGA curves of (A) catechin and (B) Au@PC NPs.

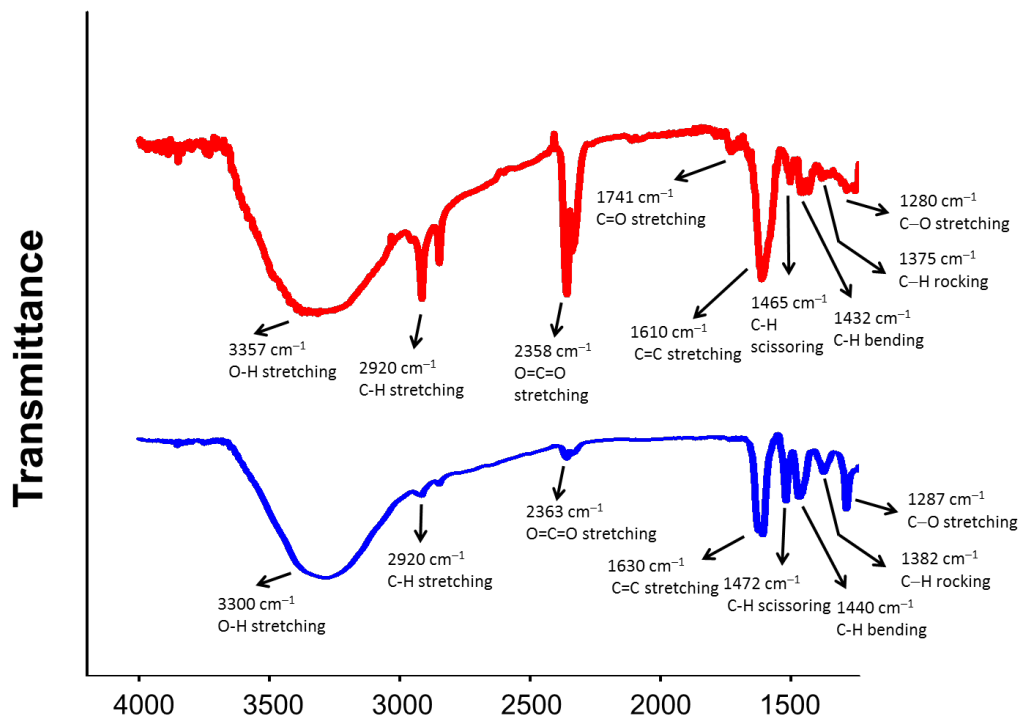


Figure S7. FT-IR spectra of catechin (blue) and purified Au@PC NPs (red).

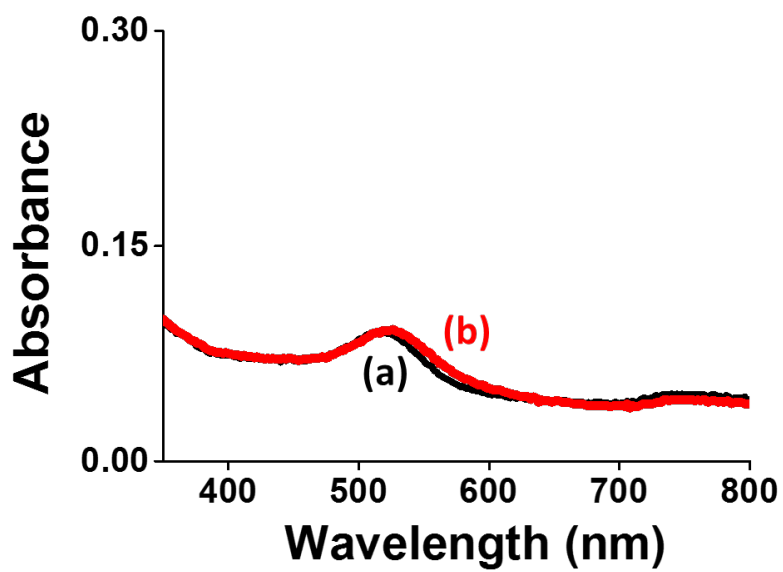


Figure S8. UV-vis absorption spectra of as-prepared AS1411-Au NPs (10-fold diluted) incubated in (a) DI water and (b) 2-fold diluted human plasma for 2 h.

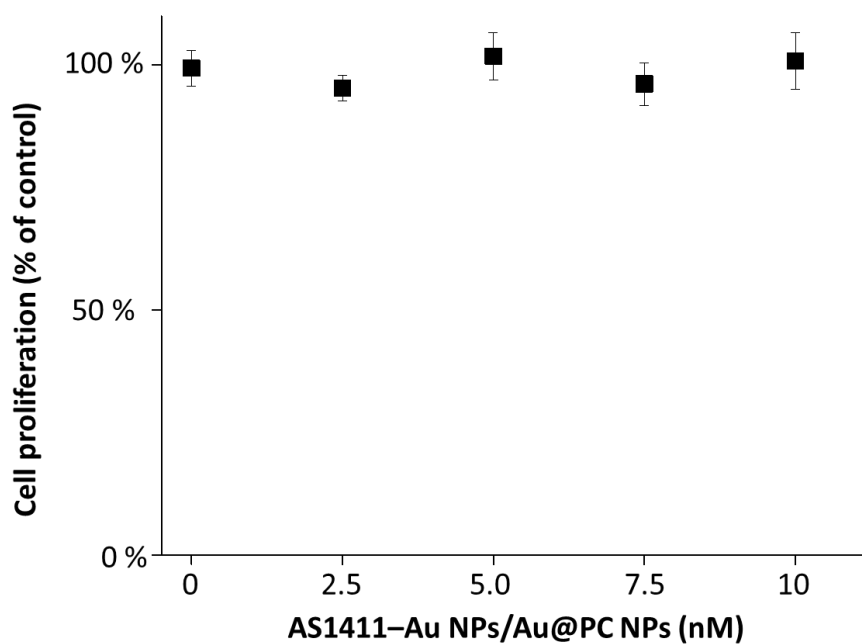


Figure S9. Cell viability of MCF-10A cells (1.0×10^4 cells well⁻¹) after treated with AS1411-Au NPs/Au@PC NPs ([AS1411-Au NPs] = 0–10 nM) in culture media at 37 °C for 24 h. Error bars represent the standard deviation of three repeated measurements.

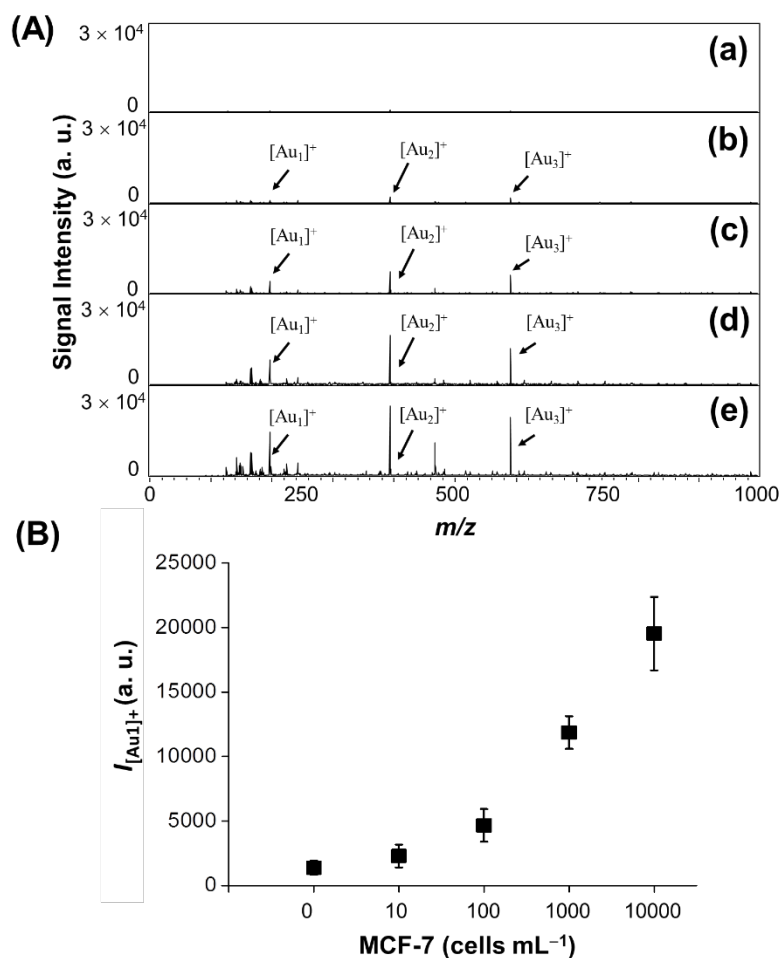


Figure S10. (A) LDI mass spectra recorded using AS1411–Au NPs/Au@PC NP as a probe for the detection of (a) 0, (b) 10, (c) 100, (d) 1000, and (e) 10,000 MCF-7 cells mL⁻¹. (B) Plots of the [Au₁]⁺ intensity ($I_{[Au_1]^+}$) with respect to the concentration of MCF-7 cells (0–10,000 cells mL⁻¹). A total of 1000 pulsed laser shots were applied to accumulate the signals from five LDI-targeted positions at a laser power density of 5.0×10^4 W cm⁻². Peak intensities in (A) and the intensities of the signals for [Au₁]⁺ in (B) are plotted in arbitrary units (a. u.). The error bars in (B) represent standard deviations from five repeated measurements. Other conditions were the same as those described in Figure 4.

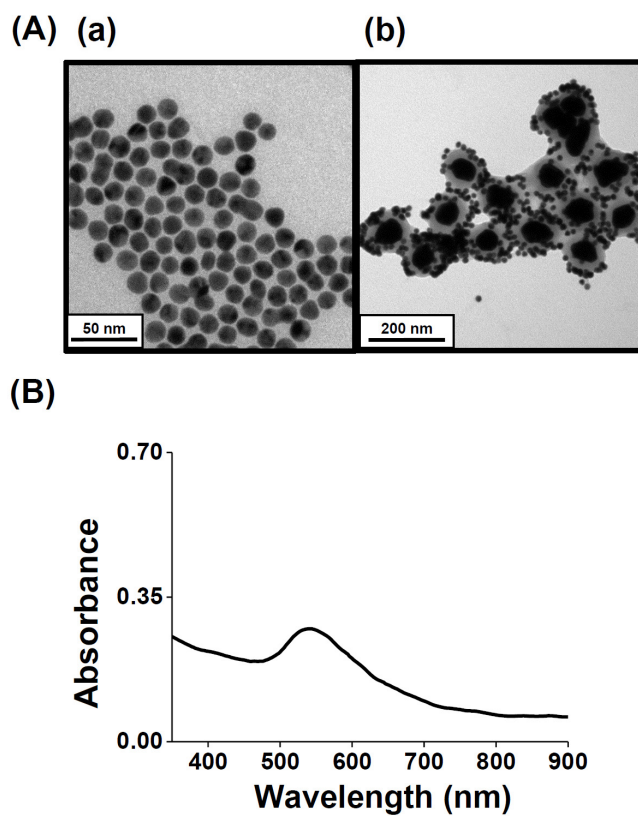


Figure S11. (A) TEM images of as-prepared (a) rDNA–Au NPs and (b) rDNA–Au NPs/Au@PC NP nanocomposites. (B) UV-vis absorption spectra of rDNA–Au NPs/Au@PC NP prepared in PBS.

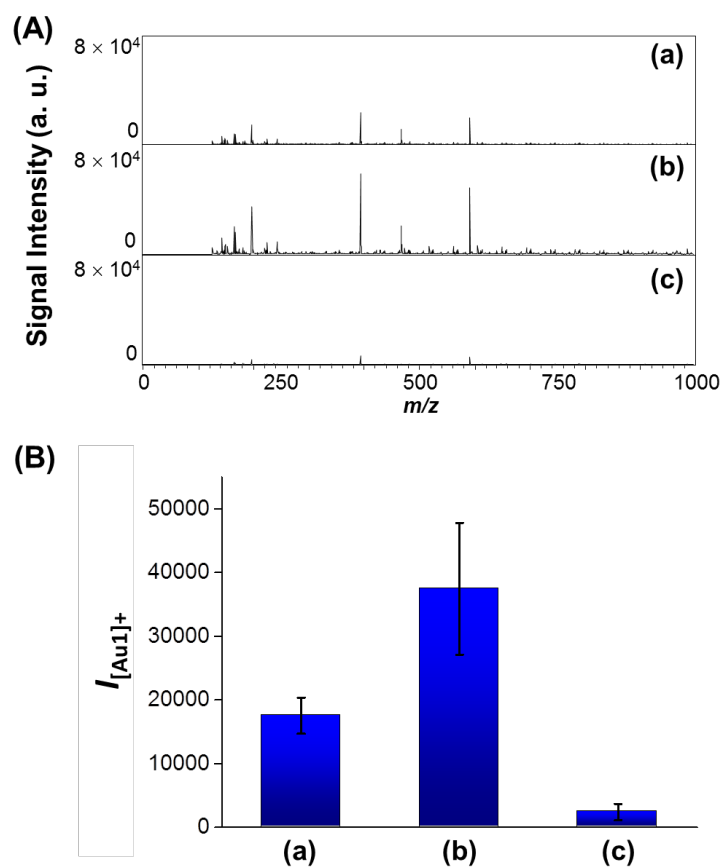


Figure S12. (A) LDI mass spectra recorded using AS1411–Au NPs/Au@PC NP as a probe for the analysis of (a) MCF-7, (b) MDA-MB-231, and (c) MCF-10A (10^4 cells mL^{-1}). (B) Peak intensities of $[\text{Au}^+]$ ions ($I_{[\text{Au}]^+}$) obtained from AS1411–Au NPs/Au@PC NP-labeled (a) MCF-7, (b) MDA-MB-231, and (c) MCF-10A. Error bars represent standard deviations from five repeated measurements. Other conditions were the same as those described in Figure 4.

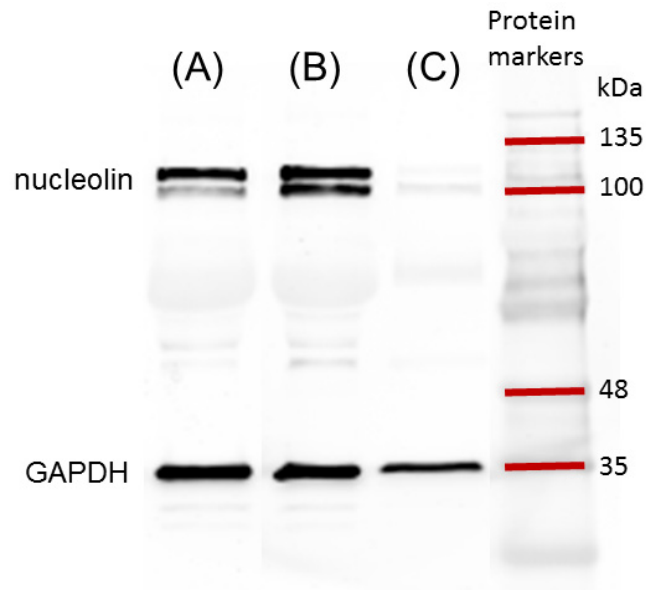


Figure S13. Western blotting for nucleolin in the cell lysates of (A) MCF-7 cells (10^5 cells well⁻¹), (B) MDA-MB-231 cells (10^5 cells well⁻¹), and (C) MCF-10A cells (10^5 cells well⁻¹).

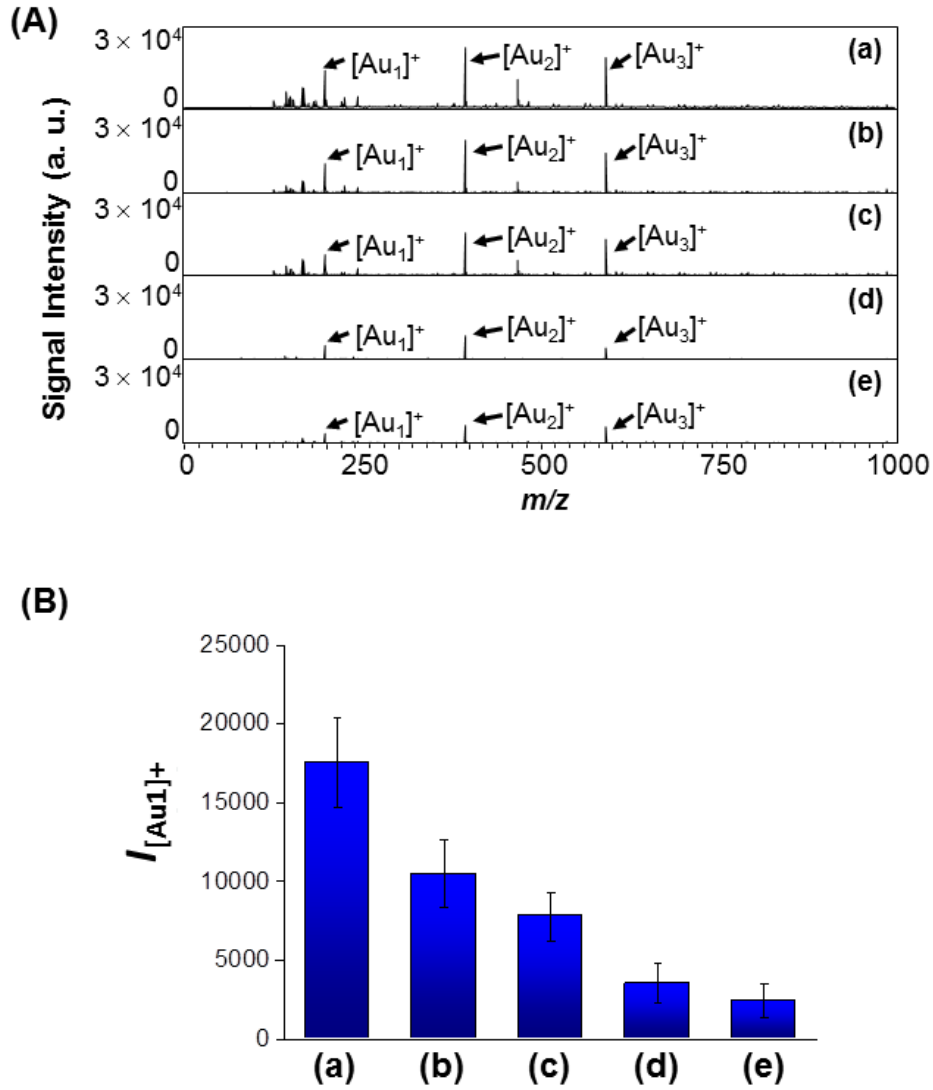


Figure S14. (A) Mass spectra recorded using AS1411–Au NPs/Au NPs@PC as a probe for the analysis of co-cultures of MCF-7 and MCF-10A cells at ratios of (a) 10 : 0, (b) 7.5 : 2.5, (c) 5 : 5, (d) 2.5 : 7.5, and (e) 0 : 10. (B) Peak intensities of $[Au_1]^+$ ions obtained after various ratios of cell numbers of MCF-7 to MCF-10A in the culture samples were labeled with AS1411–Au NPs/Au NPs@PC. Other conditions were the same as those described in Figure 4.

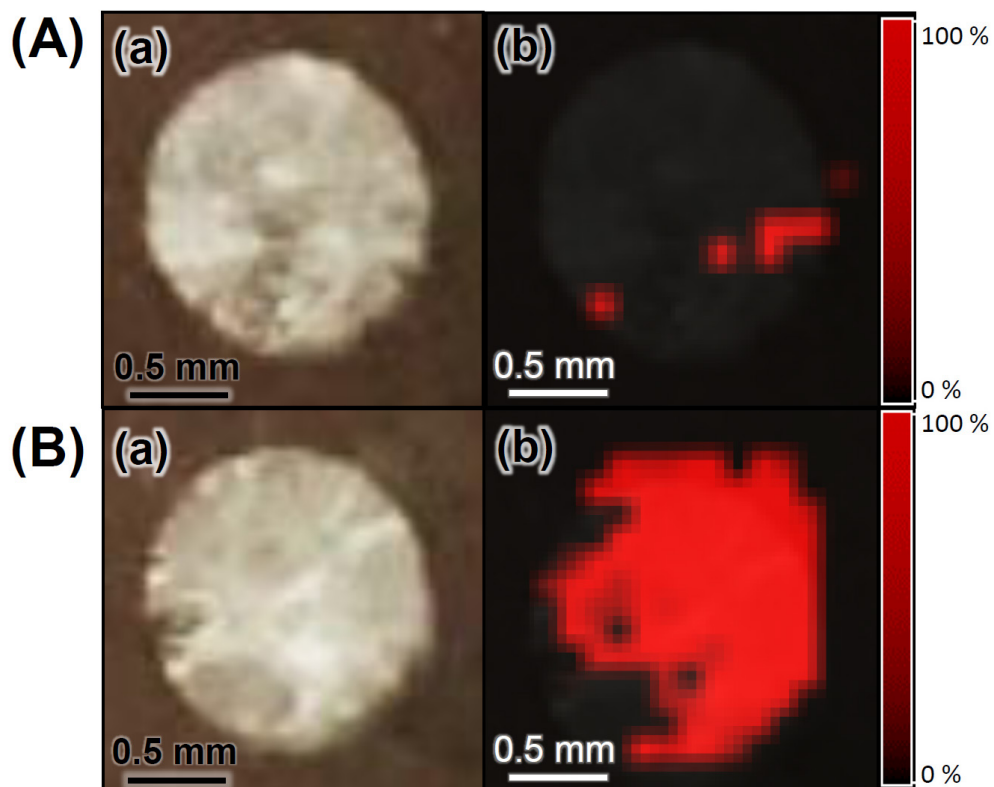


Figure S15. (a) Optical images of (A) normal breast and (B) breast tumor tissues. (b) LDI-MS images of the $[Au_1]^+$ intensity distributions in (A) normal breast and (B) breast tumor tissues after labeled with AS1411–Au NPs/Au@PC NPs. Other conditions were the same as those described in Figure 5.